Chapter 7
Modeling Single Cells in Systems Biology

Nicolai Fricker and Inna N. Lavrik

Abstract One of the most powerful methods to study the dynamic behavior of protein networks is a single-cell analysis. Introduction of fluorescent proteins provided phenomenal approach to follow living cells in the spatiotemporal manner. In this chapter we shall discuss major principles and tools used in single-cell analysis of apoptotic cells. To understand why single-cell analysis is so important, we shall compare advantages and disadvantages of single-cell versus bulk measurements. Furthermore, we shall discuss the models based on the live cell imaging and information that can be obtained with these models. In particular, we shall focus on the studies devoted to the dynamics of caspase activation and mitochondrial outer membrane permeabilization.

N. Fricker
Institute of Bioinformatics and Systems Biology, Helmholtz Zentrum München, Ingolstädter Landstraße 1, 85764 Neuherberg, Germany

Division of Immunogenetics, German Cancer Research Center (DKFZ), Heidelberg 69120, Germany

Bioquant, Heidelberg 69120, Germany

I.N. Lavrik (✉)
Department of Translational Inflammation Research, Institute of Experimental Internal Medicine, Otto von Guericke University, Leipziger Str. 44, 39120 Magdeburg, Germany
e-mail: inna.lavrik@med.ovgu.de

I.N. Lavrik (ed.), *Systems Biology of Apoptosis*, DOI 10.1007/978-1-4614-4009-3_7,

7.1 Introduction

Single cells of a genetically homogeneous cell population respond differently upon perturbation with a stimulating agent (Spencer et al. 2009). Stimulation of a cell population with death receptor (DR) ligand, for instance, will only induce death in a fraction of cells, whereas some cells will survive. There are a number of reasons for this nongenetic cell-to-cell variability. One of them is the phase within the cell cycle, which a particular cell has. A drug which induces DNA damage in S phase does not harm cells in G1 or G2 phase. Furthermore, even cells of a synchronized clonal population will show cell-to-cell variability. Sources of nongenetic cell-to-cell variability are cell size, cell density, stochastic fluctuations of biochemical reactions, and differences in the expression levels of proteins.

During the last years especially stochastic differences in protein expression have been investigated. The expression level of any protein is not identical among the cells of any cell population but rather forms a log-normal distribution as shown in Fig. 7.1 (Spencer et al. 2009). The expression level of a particular protein among cells of a clonal population can vary about 2.5-fold. This is not only true for cancer cells in culture but also for human tissue (Spencer et al. 2009). Where are these differences coming from? One of the sources of variations results from the differences at transcription level. In one cell there might be but few transcription initiating complexes, in some cells only one or two (Raj and van Oudenaarden 2008). Therefore, stochastic effects could lead to differences in gene transcription among single cells. Fluctuations in transcribed mRNA levels would result in differences in protein amounts. Naturally differences in protein amounts may give rise to differences in the response of the cells.

What might be the biological purpose of this nongenetic cell-to-cell variability? Sorger and Spencer suggest that this will give the human body a possibility to scale the response to a death stimulus (Spencer and Sorger 2011). For example, a certain amount of CD95L could induce death in a certain fraction of cells. If nongenetic cell-to-cell variability would not occur, either all or none of the cells would die. However, as cell-to-cell variability exists, the body can choose to induce cell death in, for example, 30% of all cells of a certain type. To induce apoptosis to a higher extent of the same population, the concentration of the death-inducing agent should be increased.

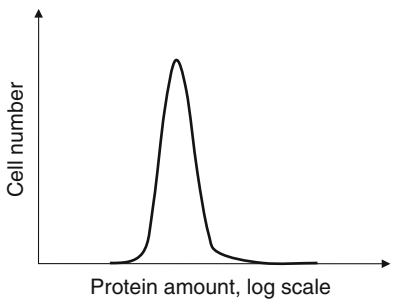

Fig. 7.1 Log-normal distribution of protein expression levels. The figure shows a scheme of the distribution of the expression level of a protein within a clonal population

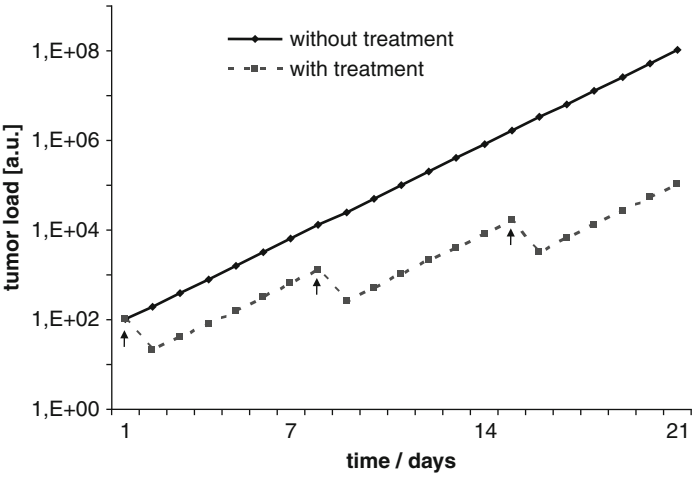

Fig. 7.2 Cell-to-cell variability contributes to tumor resistance. The *black curve* shows simulated tumor growth without treatment. The *gray dashed curve* displays tumor growth upon weekly treatment. *Arrows* indicate application of treatment. Cells in this model divide once per day. A single dose of treatment eliminates 90% of the tumor cells

While this interpretation is a pure speculation, the consequences of nongenetic cell-to-cell variability for treatment of cancer patients are of high importance. Upon treatment with a drug which should eliminate cancer cells, it is well documented that only a fraction of these cells would respond. A simple calculation shows that the assumption of only small difference in protein amounts, leading to the unresponsiveness of the marginal fraction of cells, might explain the absence of response to the treatment at the population level. Indeed, if one considers that upon treatment with a particular drug 10% of tumor cells would survive due to a nongenetic variability, then this particular drug would kill only 90% of tumor cells upon each application. Furthermore, taken that tumor cells divide once per day and the drug is applied once per week, this treatment could not control tumor growth in a patient—even in the absence of resistant stem cells or mutations! In the time interval during the application of treatment, more tumor cells will grow than will be killed by the drug (Fig. 7.2). This example demonstrates that to understand the population response, it is essential to follow the single cells. Therefore, it is of high importance to model the behavior of not only a certain tissue or cell type, but also of single cells.

7.2 Single-Cell and Bulk Measurement Techniques

To model protein networks two types of quantitative experimental data could be used: bulk measurements and single-cell analysis. In the following we will compare these two types of experimental data.

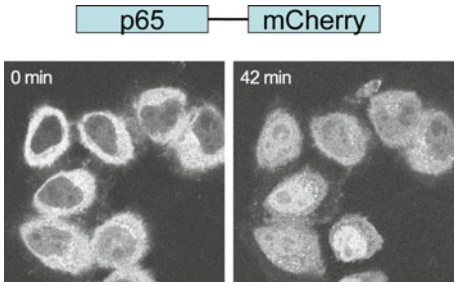

Fig. 7.3 Measuring NFκB localization with a p65-mCherry fusion protein. A scheme of the p65-mCherry fusion protein is displayed on *top*. *Bottom*: p65-mCherry is mainly found in the cytosol in non-stimulated cells. Forty-two minutes after CD95 stimulation with 1 μg/ml of agonistic anti-APO-1 antibody, p65-mCherry translocates into the nucleus. Modified from Neumann et al. (2010)

The most commonly used bulk measurement technique for protein amounts, their activity, and modifications is Western blotting (WB). It allows to determine the average protein amounts as well as cleavage, phosphorylation, or other protein modifications in a cell population (Schilling et al. 2005). WB is often combined with immunoprecipitations which allows to purify and analyze protein complexes. The principle is that the protein of interest can be detected with specific antibodies and further quantified using fluorescence or luminescence measurements. Furthermore, the number of proteins that could be detected simultaneously is unlimited if corresponding antibodies are available. The WB allows to follow the change in protein amounts, kinetics of protein modifications, and formation of protein complexes in the cell. However, WB is not applicable for single-cell measurements as the protein amounts produced by one cell are much too low to be detected.

Another method which can be considered as a bulk measurement is flow cytometry. In flow cytometry cells are marked or stained with fluorescent molecules or antibodies. This allows to determine the amount of particular protein in these cells. Several proteins may be measured simultaneously. In the field of cell death, a standard application of flow cytometry is determining the amount of dead or apoptotic cells in response to treatment. However, a disadvantage of this technique is that it is impossible to follow one single cell over a period of time. Flow cytometry rather takes a snapshot of a cell population at a certain time point. This disadvantage can be overcome with live imaging of a single cell.

Fluorescent tagging of proteins or probes has provided a remarkable insight into cellular processes. A protein can be fused to green fluorescent protein (GFP) or other fluorescent protein, which would yield information about the localization and amount of the fusion protein. This gives a unique way for tracking living cells, organelles, and even single molecules in the spatiotemporal manner. Following localization, fluorescent protein could be used as a functional readout for many cellular processes. For example, NFκB activation could be monitored by live cell imaging, e.g., NFκB nuclear translocation could be visualized using a p65-mCherry construct (Neumann et al. 2010) (Fig. 7.3).

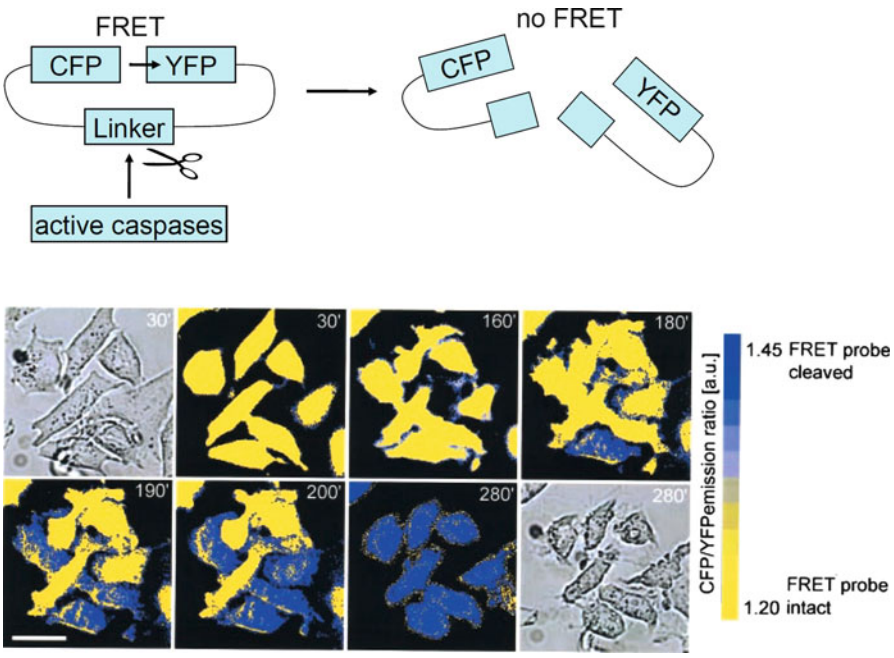

Fig. 7.4 Measuring caspase activity with FRET probes. *Top*: A scheme of a FRET caspase activity probe. It consists of two fluorophores linked by a peptide containing the cleavage sequence of a specific caspase. Upon cleavage of the linker by caspases, the fluorophores separate and the FRET signal is lost. *Bottom*: Loss of FRET signal of a caspase-3 activity probe as determined in HeLA cells upon stimulation with 3 μM staurosporine. Modified from Rehm et al. (2002)

Another method to visualize cellular events is the usage of activity probes, which typically comprise fluorescent proteins and could be modified by protein activity. In the field of apoptosis, activity probes are mostly constructed in a way such that they contain caspase cleavage site, which is cleaved upon caspase activation. Hence, these probes could be implemented to detect caspase activation and thereby apoptosis induction. One of the first caspase activity probes has been constructed by Rehm and coworkers (Rehm et al. 2002). It comprises two fluorophores, which could generate Foerster resonance energy transfer (FRET) signal. Two fluorophores are separated by the caspase cleavage site (Fig. 7.4). Without apoptosis induction the probe produces a constant FRET signal. Upon cleavage of the probe by caspases, the two fluorophores of the probe get separated and the FRET signal disappears (Fig. 7.4). In this way the decrease in FRET signal serves as readout for caspase activity.

Another way to determine caspase activity in single cells is to construct localization probes. The elegant localization probe was constructed by Joel Beaudouin (Fricker et al. 2010). It consists of a nuclear export signal linked to the cleavage sequence of a caspase fused to mCherry. In resting cells, the probe localizes to the

Table 7.1 Fluorescent probes that could be used to measure single cells

Type	Description	Example
Fusion proteins	A protein fused to a fluorescent molecule (e.g., GFP, YFP, CFP, mCherry, and others)	p65-mCherry (Neumann et al. 2010) (Fig. 7.3)
FRET probes	Two fluorophores are kept in proximity by a linker. Modification of the probe abolishes or enhances the FRET signal	Caspase-3 activity probe (Rehm et al. 2002). Cleavage of the linker by caspases separates the fluorophores, leading to the loss of the FRET signal (Fig. 7.4)
Localization probes	A target sequence fused to a fluorescent protein via a linker	A nuclear export signal fused to the linker peptide sequence IETD fused to mCherry. Cleavage of the linker by caspases separates the fluorescent protein from the target sequence. The fluorescent protein then freely diffuses and translocates into the nucleus (Fricker et al. 2010)

cytoplasm due to the nuclear export signal. Upon cleavage by caspases, nuclear export signal is cleaved off and mCherry translocates to the nucleus. Using fluorescent probes and live cell imaging, it is possible to follow the response of a single cell for hours or even for days. Table 7.1 summarizes different fluorescent probes that could be used in the field of apoptosis to measure single cells.

One might ask why WB is still used in quantitative biology and not exclusively live cell imaging. Fluorescent reporters have some disadvantages: The number of reporters that can be visualized simultaneously is, of course, limited. At some point the fluorescent spectra of the multiple fluorophores used will overlap. Furthermore, usage of a reporter requires manipulation of the respective cell. Introduction of the reporter or the reporter itself may alter cellular behavior. These limitations do not apply for WB. In addition, the formation of several cleavage products may be measured quite easily with WB. For instance, generation of the caspase cleavage products can be detected using WB. With fluorescent microscopy, there is no simple way to observe this. Therefore, it is always an optimal strategy to combine bulk measurements and single-cell experiments.

7.3 Relying Exclusively on Bulk Data Might Result in Wrong Interpretations

It is impossible to accurately model single-cell behavior when relying on bulk measurements exclusively. This can be shown with an example. In a bulk measurement, one could see a continuous and slow increase in protein concentration, for instance, of cleaved caspase-3 (Fig. 7.5a). Do the single cells display the same behavior? Not necessarily. Figure 7.5b shows two examples of responses of single

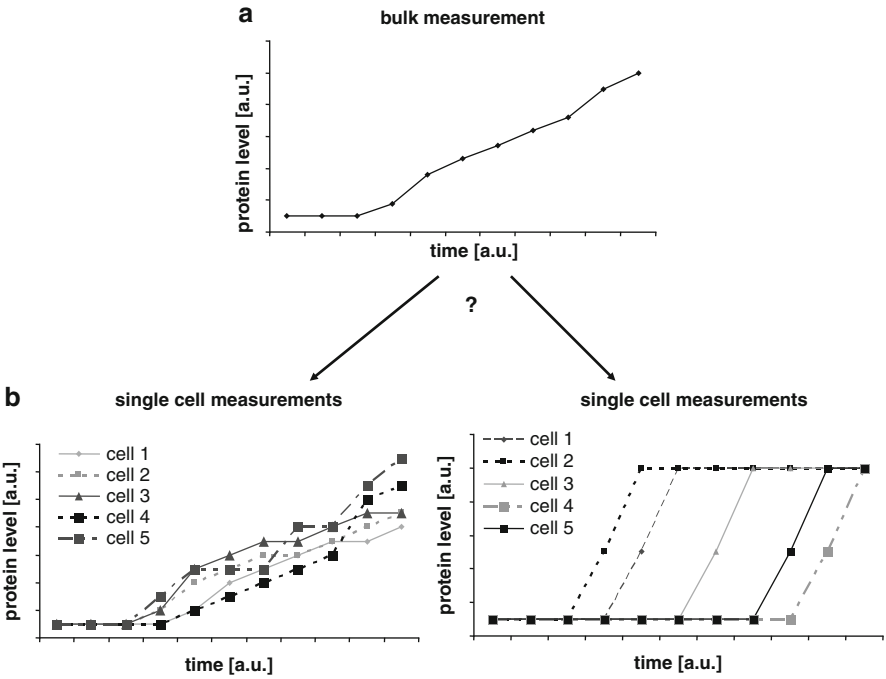

Fig. 7.5 Single-cell behavior cannot be recovered from bulk measurements. (**a**) Example of protein amounts determined in a bulk measurement. (**b**) Two examples of how single cells could behave resulting in the same bulk measurement data as shown on *top*

cells, which could result in the same bulk measurement. They look quite different. On the left-hand side of Fig. 7.5b, single cells display a slow and gradual increase in the amount of the protein. On the right-hand side, single cells show a variable lag time followed by a rapid response. Therefore one might draw wrong conclusions relying exclusively on WB.

Another example of events which are not feasible to analyze using bulk measurements are oscillations. For example, p53 oscillations were reported to occur upon DNA damage (Loewer et al. 2010). Figure 7.6 shows an example, which includes a bulk measurement and the corresponding single-cell data. In this case oscillations within single cells disappear in the bulk measurement. This is due to the fact that cells do not respond synchronously. Relying on bulk measurements, it is not possible to determine whether two events take place in the same or in different cells. Upon CD95 stimulation phosphorylation of IκBa and cleavage of procaspase-8 can be measured using WB (Fig. 7.7a). Does one cell induce apoptosis whereas another one decides to activate NFκB? Only with help of a fluorescent NFκB reporter our group could show that both pathways are indeed activated simultaneously in the same cell (Neumann et al. 2010) (Fig. 7.7b).

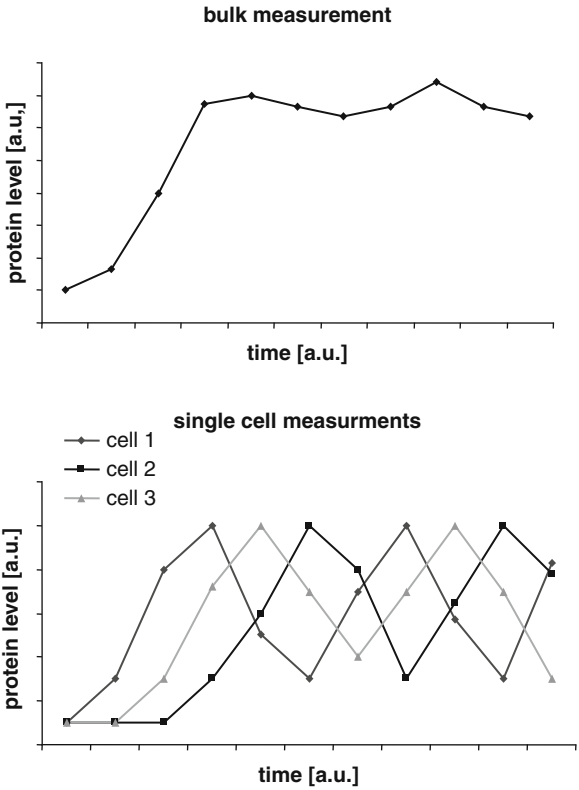

Fig. 7.6 Oscillations can be lost in bulk measurement. *Left*: Experimental data that could be obtained from a bulk measurement. There is no oscillation visible. *Right*: Single cells show oscillations. Building the mean value of the single-cell data will result in the bulk data as shown on the *top*

7.4 Modeling Single Cells

There are several considerations one has to take into account when modeling single cells in comparison to building models on bulk data. In the optimal case one knows the mean protein amounts of the main signaling molecules within a given population. These data can be directly put as initial protein concentrations into a model based on bulk measurement data. This rule does not apply to generation of models based on a single-cell analysis. One does not know the protein concentrations in a single cell. Furthermore, the protein amounts within the single cell might be 2.5 times higher or lower than the average amount within the population. Therefore, protein amounts of single cells have to be estimated. As a consequence single-cell modeling is more computationally demanding than population modeling. To fit ODE models to measurement data obtained from single cells, hundreds of

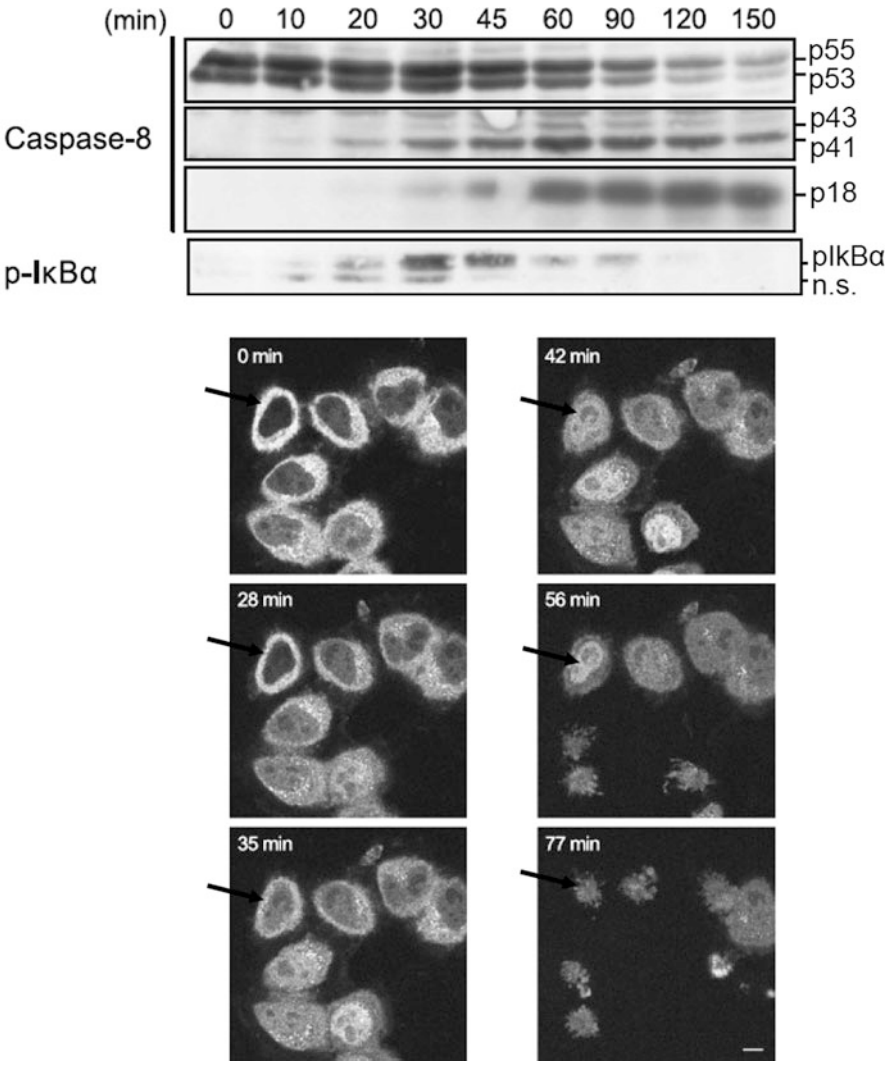

Fig. 7.7 Simultaneous activation of both NFκB and caspase-8. *Top*: Cleavage of caspase-8 and phosphorylation of IκBa as determined by WB upon stimulation of HeLa-CD95 cells with agonistic anti-APO-1 antibody. *Bottom*: Single-cell data of p65-mCherry transfected HeLa-CD95 cells upon stimulation with anti-APO-1. Nuclear localization of p65-mCherry precedes apoptosis. Modified from Neumann et al. (2010)

measurements of single cells have to be used. The protein amounts of each of these cells have to be guessed. This can be very time consuming.

In the following we will compare fitting of models based on bulk measurements to those based on single-cell data: We denote $\vec{c}(0)$ as the initial protein concentrations, t as the time, $\vec{s}$ as the experimental conditions (for example, stimulation), and $\vec{k}$ as the rate constants. A model $f : (\vec{c}(0), t, \vec{s}, \vec{k}) = \vec{c}$ yields protein amounts,

modifications, or other outputs at a given time point upon stimulation $\vec{s}$. Measurement values are given as tuples $m_{i,j} = \langle \vec{s}_i, t_j, \vec{c}_{i,j} \rangle$. $\vec{C}_{i,j}$ denotes the measured protein amounts/modifications upon stimulation $\vec{s}_i$ and time t_j. For the sake of simplicity, we assume there was only one measurement value per condition and time point. In order to fit the model, we try to minimize: $\sum_{\forall i,j:\exists m_{i,j}} \left(f(\vec{c}(0), t_j, \vec{s}_i, \vec{k}) - p(3, m_{i,j})\right)^2$, where $p(i,x)$ is the projection of the tupel x to the ith dimension. In case the mean initial protein amounts as well as their modifications are known, only the rate constants $\vec{k}$ have to be estimated. However, for modeling single cells, we have to take into account that single cells possess different protein amounts. We will denote the initial protein concentrations of a cell n as $\vec{c}_n$. In order to fit the model, we would have to minimize: $\sum_{\forall n,i,j:\exists m_{i,j,n}} \left(f(\vec{c}_n(0), t_j, \vec{s}_i, \vec{k}) - p(4, m_{i,j,n})\right)^2$ with $m_{i,j,n} = \langle \vec{s}_i, t_j, n, \vec{c}_{i,j,n} \rangle$. Like for the model based on bulk measurements, we have to estimate the rate constants $\vec{k}$. However, additionally the initial protein concentrations or the initial state of the cells have to be estimated locally, too. Term "locally" means that these values are estimated for each cell and vary between cells. This type of task could be performed by software like, for example, "potterswheel." For large amounts of cells, the distribution of the initial protein amounts should approximate a log-normal distribution like the one shown in Fig. 7.1. In contrast, rate constants must be identical in all cells. They have to be estimated globally. In comparison to fitting to bulk data, fitting to single-cell data will be more time consuming and the model parameters might be less determined, as additional unknown variables are introduced. If the resulting model is simulated several hundred or thousand times with varying initial conditions according to a log-normal distribution as shown in Fig. 7.1, then the sum of the simulations outputs will mimic a bulk measurement. Therefore, a model based on single-cell data is capable of predicting the output of bulk experiments and can be challenged as well as verified in this way. However, a model based exclusively on bulk data will in many cases not be able to describe single-cell behavior accurately. Often, however, the topology which was identified when constructing a model on bulk measurements might be the same.

7.5 Caspase-3 Activation in Type II Cells: A Case Study

An example of how single-cell measurements can be applied in systems biology is the modeling of activation of caspase-3 in type II cells. Groups of Jochen Prehn and Peter Sorger made a significant contribution to unravel this question. Upon DR stimulation the death-inducing signaling complex (DISC) is formed. Procaspase-8 is activated at the DISC. Following procaspase-8 activation at the DISC, apoptotic signaling can go via type I or type II, which is described in detail in Chap. 5. Type I cells are characterized by high levels of DISC formation and high amounts of active caspase-8. Activated caspase-8 directly leads to activation of downstream effector caspases-3 and -7. In type II cells, there are lower levels of DISC formation and, thus, lower levels of active caspase-8. In this case, comprising the majority of cell

lines, signaling requires an amplification loop. This amplification loop involves the cleavage by caspase-8 of the Bcl-2 family protein Bid to generate truncated (t) Bid and subsequent tBid-mitochondrial outer membrane permeabilization (MOMP). Only after mitochondrial outer membrane permeabilization (MOMP), caspase-3 is fully activated and apoptosis is initiated. This was shown using FRET reporter capable of measuring caspase-3 activity by Rehm et al. (2002). Upon cleavage of the reporter by caspase-3, the FRET signal is diminished as the interaction between the fluorophores of the probe is lost. Figure 7.8a shows caspase-3 activity as measured in a bulk experiment. Figure 7.8b displays the kinetic of FRET probe cleavage in single cells treated with TNF-α. In the bulk experiment it seems that there is a slow and steady increase over time. However, single-cell data reveal that the actual behavior is different. There is a lag time after stimulation with TNFα. In this time interval, no change in probe fluorescence can be detected. This lag time was also termed pre-MOMP delay. The duration of the lag time greatly varies between single cells. The lag phase is followed by a rapid cleavage of the probe. Within 10 min, complete processing of the probe takes place. This is independent of the stimulus strength used to induce MOMP (Fig. 7.8). The activation of caspase-3 follows an all-or-none behavior. Other groups made the same observation (Goldstein et al. 2000; Tyas et al. 2000). Either no substrate cleavage occurs or all substrates are rapidly cleaved. Interestingly MOMP preceded activation of caspase-3 by 10 min.

Rehm and colleagues found that probe processing could be well described by the following equation: $c(t) = f - \frac{f}{1+e^{(t-Td)/4Ts}}$.

In this equation $c(t)$ is the amount of cleaved substrate at time t, f is the fraction cleaved at the end of the reactions, and Td is the delay between stimulation and the half-maximal substrate cleavage. Ts is the switching time between initial and complete effector substrate cleavage. In 2006 the same group combined the caspase-3 activity probe measurements with tetramethyl rhodamine ethyl ester (TMRM), a marker of the mitochondrial potential. Based on these data, a model describing caspase-3 activation upon MOMP was built (Fig. 7.9). Applying sensitivity analysis, the authors identified procaspase-9, -3, and the XIAP concentrations as the main factors which determine rapid caspase-3 activation following MOMP. There are two reasons for the all-or-none behavior of caspase-3. First, cleaved and thereby activated caspase-3 is counteracted by XIAP. Hence, when the amount of the active caspase-3 is above the one that could be blocked by XIAP, the caspase-3 activation could not be blocked anymore. Second, as soon as cyt c is released, the apoptosome is being formed, and caspase-9 is activated. A positive feedback between caspase-3 and caspase-9 is turned on, which leads to rapid caspase-3 activation. The authors predicted that MOMP-induced apoptosis initiation will be slowed down upon XIAP overexpression and could confirm this prediction experimentally. Moreover, overexpression of XIAP could lead to sublethal caspase activation and incomplete substrate cleavage. This has been proposed to promote tumor formation.

Two years later the group of Peter Sorger came up with a larger model describing both caspase-8 and subsequent caspase-3 activation upon TRAIL stimulation (Fig. 7.10) (Albeck et al. 2008b). This was the first model based on single-cell data

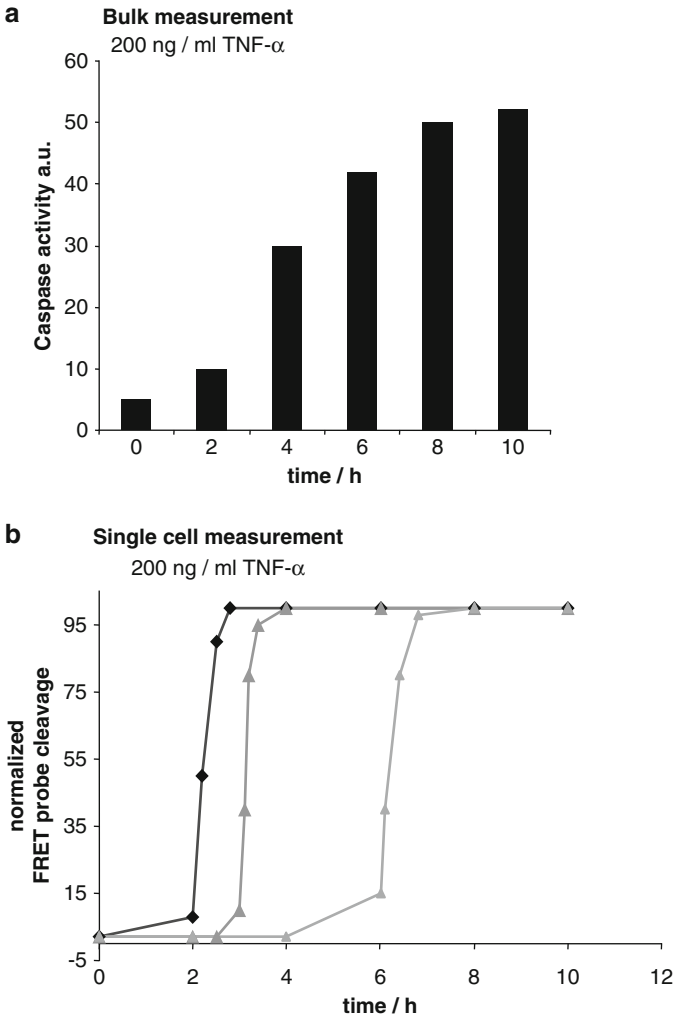

Fig. 7.8 Kinetics of effector caspase activation upon TNF-α stimulation. (**a**) Caspase-3 activity as determined by DEVD cleavage upon stimulation of HeLA cells with TNF-α plus cycloheximide. Bulk measurements suggest a gradual increase in activity. (**b**) Caspase-3 activity as determined in single cells with a FRET probe. Processing of the FRET probe occurs rapidly after a lag phase of variable length. Modified from Rehm et al. (2002)

combining both the extrinsic and the intrinsic pathways. The authors used probes which could specifically be cleaved by either caspase-8 (termed initiator caspase reporter protein, IC-RP) or caspase-3/7 (termed effector caspase reporter protein, EC-RP). Using the caspase-8-specific probe, it was demonstrated that caspase-8 activity gradually builds up at the time before MOMP termed pre-MOMP. The onset of caspase-3 activity, however, occurred after cyt c release (Fig. 7.11a)

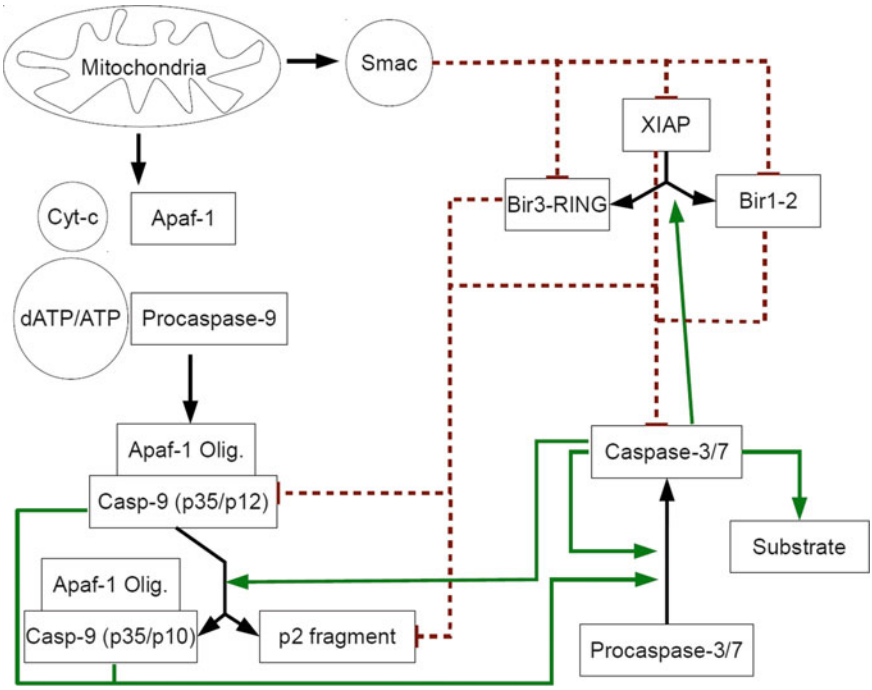

Fig. 7.9 A model of caspase-3/-9 activation upon MOMP. A scheme of a model of caspase-3 and -9 activation following MOMP. Enzymatic cleavage is indicated by *green arrows*. Inhibitory reactions are shown as *red lines*. Modified from Rehm et al. (2006)

(Albeck et al. 2008a). The variable delay in the onset of caspase-3 activity among single cells could be mainly explained by differences in initial caspase-8 activity among single cells. In addition, Smac was identified as an important regulator of rapid caspase-3 activation. As soon as MOMP occurs, Smac is released from the mitochondria leading to XIAP degradation, thereby allowing caspase-3 activation. In a series of experiments, the authors could confirm the proposed mechanism of a rapid switch from inactive to active caspase-3, which the authors termed "snap-action of caspase-3" activation:

1. The authors proposed that procaspase-3 was cleaved before MOMP, however, rapidly inactivated by XIAP. Therefore, XIAP depletion should abolish this inhibition and allow effector caspase activity before MOMP. Indeed, simultaneous depletion of both Bid (in order to prevent MOMP) and XIAP resulted in a gradual increase in EC-RP cleavage upon stimulation (Fig. 7.11b).
2. Upon MOMP Smac is released from the mitochondria leading to XIAP degradation. This would abolish the caspase-3 inhibition by XIAP and contribute to snap-action of caspase-3 activation. The Albeck model predicted that upon Smac down-regulation, caspase-3 activity would increase more slowly following

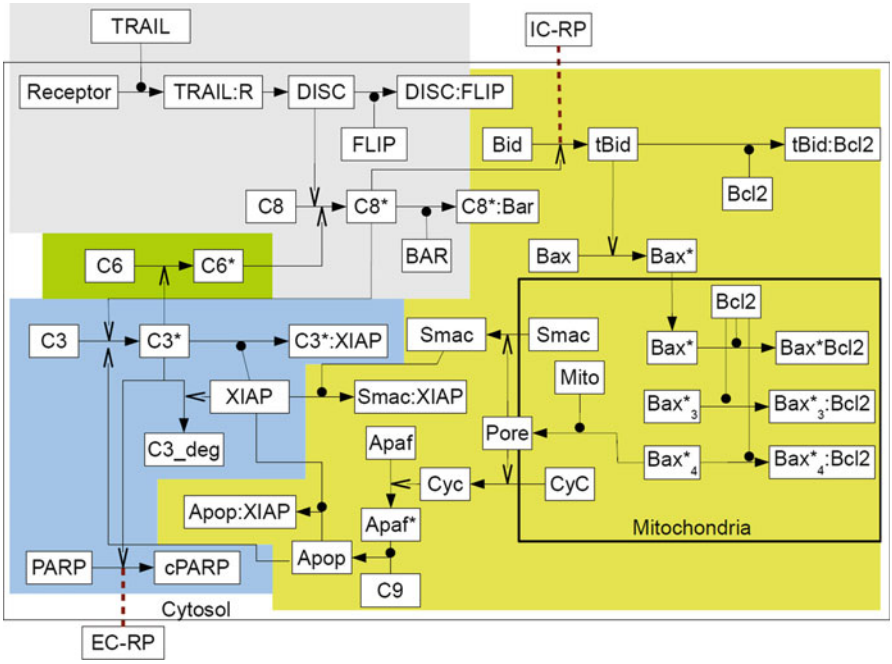

Fig. 7.10 A model of the TRAIL signaling pathway. A scheme of the TRAIL signaling pathway. *Symbols* in the scheme follow the convention of Kitano et al. *Background colors* indicate different network modules. Modified from Albeck et al. (2008b)

MOMP. This prediction could be confirmed experimentally: Upon Smac knockdown, a gradual increase in effector caspase activity occurred (Fig. 7.11c).

The Albeck model was able to reproduce both single-cell and WB data accurately. It consists of 70 rate constants and 98 species. Interestingly, the model parameters were taken from the literature as well as fitted manually. The model nicely proposed a mechanism for the all-or-none behavior observed with respect to caspase-3 activation. All-or-none behavior of effector caspase activation is an important property, as it establishes MOMP as a point of no return. MOMP leads to full activation of caspases-3 and -9 and cell death.

7.6 Investigation of Nongenetic Cell-to-Cell Variability in the TRAIL Pathway

Spencer et al. (2009) investigated nongenetic cell-to-cell variability. The authors found that the phase within the cell cycle or cell size barely influences the mean time to MOMP upon TRAIL stimulation (Spencer et al. 2009). However they discovered that sister cells shortly after cellular division behaved very similarly. Similarity

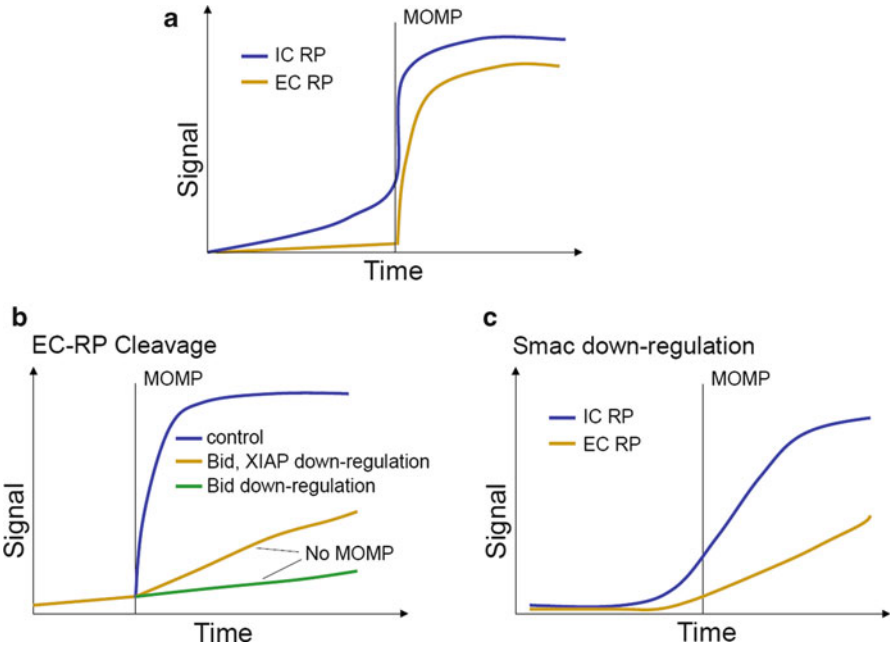

Fig. 7.11 Snap-action of caspase-3. (**a**) Cleavage of IC-RP and EC-RP in HeLa cell treated with 50 ng/ml TRAIL plus 2.5 μg/ml cycloheximide. Caspase-8 activity (IC-RP) gradually increases until MOMP. Caspase-3 activity (EC-RP) is absent before MOMP. Cells are aligned by the average time of MOMP. (**b**) EC-RP cleavage upon down-regulation of Bid or Bid plus XIAP. Bid down-regulation will prevent MOMP. Upon co-down-regulation of XIAP, a gradual increase in probe cleavage is observed. (**c**) Cleavage of EC-RP and IC-RP upon Smac down-regulation. Upon down-regulation of Smac, snap-action of caspase-3 is abolished. Instead a gradual and slow increase in caspase-3 activity is observed. Modified from Albeck et al. (2008b)

between sister pairs decreased with increasing time after cellular division. Directly after division two daughter cells have almost identical protein amounts and modifications. It was suggested that stochastic events during transcription could lead to different protein levels among two daughter cells. These differences would accumulate. Several hours after cellular division, two sister cells will not be more similar than any two random cells. The authors therefore proposed that random differences in protein amounts are one major source of cell-to-cell variability. The model as published by Albeck et al. (2008b) could indeed reproduce this observation. Differences in protein expression of a factor of 2.5 were sufficient to cause differences in phenotype. Another important prediction was that for the TRAIL pathway, there is not one single most important protein deciding the outcome of stimulation. If, for example, the amount of procaspase-8 is relatively high in a single cell, this does not mean that this cell is especially sensitive towards TRAIL-induced apoptosis. As there is a number of anti-apoptotic players involved, the pro-apoptotic effect of procaspase-8 might be compensated by these proteins. This prediction could be elegantly confirmed by Spencer and coauthors. A cell line was used

expressing a c-FLIP YFP fusion protein at the endogenous locus, resulting in physiological expression levels of the construct (Spencer et al. 2009). Surprisingly, no correlation was found between the expression of c-FLIP YFP in single cells and the time when MOMP occurred after TRAIL stimulation. On the basis of these observations, it was suggested that variations in the expression level of one protein are not sufficient to determine sensitivity. Whether other sources of cell-to-cell variability like, for example, protein phosphorylation might have similar impacts is an issue to be addressed in the future.

7.7 Summary and Outlook

In the previous sections, we learned how single-cell experiments could provide fascinating insights into cellular processes. They allow to investigate dynamics which cannot be detected in bulk measurements. In combination with mathematical modeling, single-cell measurements are a powerful tool to gain better understanding in the field of biology.

However, there are issues on both the modeling and the experimental side to be improved in the future. So far it has not been possible to monitor a large number of events simultaneously in a single cell. Especially FRET probes have the disadvantage that they occupy a large area of the wavelength spectrum, naturally restricting a number of proteins to be monitored with FRET probes. Measuring a larger number of cellular events in parallel would allow investigating the interplay of signaling processes. On the modeling side mostly ODEs have been applied so far with great success (Bentele et al. 2004; Albeck et al. 2008a, b; Neumann et al. 2010; Fricker et al 2010). However, as Spencer et al. (2009) showed that random fluctuations in transcription have a large impact on cellular behavior, stochastic modeling will be more and more important in the future. Especially in models in which transcription has to be incorporated, stochastic models might describe the cellular behavior more accurately. Taken together, further development of both experimental methods and modeling approaches could provide even more exciting insights into regulation of cellular decisions.

Acknowledgments We acknowledge the Helmholtz Alliance on Systems Biology (NW1SBCancer) and Helmholtz-Russia Joint Research Groups-2008-2 for supporting our work.

References

Albeck JG, Burke JM, Aldridge BB et al (2008a) Quantitative analysis of pathways controlling extrinsic apoptosis in single cells. Mol Cell 30:11–25. doi:10.1016/j.molcel.2008.02.012

Albeck JG, Burke JM, Spencer SL et al (2008b) Modeling a snap-action, variable-delay switch controlling extrinsic cell death. PLoS Biol 6:2831–2852. doi:10.1371/journal.pbio.0060299

Bentele M, Lavrik I, Ulrich M et al (2004) Mathematical modeling reveals threshold mechanism in CD95-induced apoptosis. J Cell Biol 166:839–851. doi:10.1083/jcb.200404158

Fricker N, Beaudouin J, Richter P et al (2010) Model-based dissection of CD95 signaling dynamics reveals both a pro- and antiapoptotic role of c-FLIPL. J Cell Biol 190:377–389. doi:10.1083/jcb.201002060

Goldstein JC, Waterhouse NJ, Juin P et al (2000) The coordinate release of cytochrome c during apoptosis is rapid, complete and kinetically invariant. Nat Cell Biol 2:156–162. doi:10.1038/35004029

Loewer A, Batchelor E, Gaglia G, Lahav G (2010) Basal dynamics of p53 reveal transcriptionally attenuated pulses in cycling cells. Cell 142:89–100. doi:10.1016/j.cell.2010.05.031

Neumann L, Pforr C, Beaudouin J et al (2010) Dynamics within the CD95 death-inducing signaling complex decide life and death of cells. Mol Syst Biol 6:352. doi:10.1038/msb.2010.6

Raj A, van Oudenaarden A (2008) Nature, nurture, or chance: stochastic gene expression and its consequences. Cell 135:216–26. doi:10.1016/j.cell.2008.09.050

Rehm M, Dussmann H, Janicke RU et al (2002) Single-cell fluorescence resonance energy transfer analysis demonstrates that caspase activation during apoptosis is a rapid process. Role of caspase-3. J Biol Chem 277:24506–24514. doi:10.1074/jbc.M110789200

Rehm M, Huber HJ, Dussmann H, Prehn JHM (2006) Systems analysis of effector caspase activation and its control by X-linked inhibitor of apoptosis protein. EMBO J 25:4338–4349. doi:10.1038/sj.emboj.7601295

Schilling M, Maiwald T, Bohl S et al (2005) Computational processing and error reduction strategies for standardized quantitative data in biological networks. FEBS J 272:6400. doi:10.1111/j.1742-4658.2005.05037

Spencer SL, Sorger PK (2011) Measuring and modeling apoptosis in single cells. Cell 144:926–39. doi:10.1016/j.cell.2011.03.002

Spencer SL, Gaudet S, Albeck JG et al (2009) Non-genetic origins of cell-to-cell variability in TRAIL-induced apoptosis. Nature 459:428–32. doi:10.1038/nature08012

Tyas L, Brophy VA, Pope A et al (2000) Rapid caspase-3 activation during apoptosis revealed using fluorescence-resonance energy transfer. EMBO Rep 1:266–270. doi:10.1093/embo-reports/kvd050